Inorg. Chem. **2003**, *42*, 1835–1841

Synthesis and Structure of the Metallic K_6Tl_{17}: A Layered Tetrahedral Star Structure Related to That of Cr_3Si

Stefan Kaskel,[†] Zhen-Chao Dong,[‡] Michael T. Klem,[§] and John D. Corbett*

Ames Laboratory[1] and Department of Chemistry, Iowa State University, Ames, Iowa 50011

Received November 12, 2002

The title compound, the Tl-richest in the K–Tl system, has been synthesized in Ta containers via direct reaction of the elements at 400 °C followed by quenching to room temperature and subsequent annealing at 150 °C for 4 weeks. It crystallizes in the orthorhombic space group *Cccm* (No. 66) with $a = 16.625(1)$ Å, $b = 23.594(2)$ Å, $c = 15.369(2)$ Å (22 °C), and $Z = 8$. Two different Tl_{12} units consisting of augmented tetrahedral stars are condensed into layers of such tetrahedra, and further Tl_2 dumbbells and the potassium cations also interconnect the stars and layers into a three-dimensional network. The former anionic Tl_8 subunits clearly resemble those in the heteroatomic 3-D structure of cubic Cr_3Si before their augmentation with bridging atoms. The compound is metallic ($\rho_{270} = 22.6$ $\mu\Omega$·cm, $\alpha = 0.0023$ K^{-1}) and shows Pauli-like paramagnetic susceptibility ($\chi_{296} = 1.1 \times 10^{-4}$ emu/mol). EHTB calculations illustrate the importance of Tl p-orbital bonding, the positive Tl–Tl overlap populations up to E_F, and greater strengths of the Tl–Tl bonding between and about the surface of the augmented Tl_{12} units. Cations between the thallium layers play specific and important roles in the structure.

Introduction

The particular post-transition triel elements Ga, In, and Tl exhibit a large and diverse anionic chemistry in which they form many discrete clusters as well as extended 2-D and 3-D networks, often of considerable complexity.[2,3] The lightest member gallium forms the probably strongest homoatomic bonds and mostly complex network structures, and these regularly give way to relatively more frequent isolated cluster examples on progression to thallium. The bonding in many examples can be successfully formulated as Zintl type (closed shell), sometimes with simple octet rules but more often utilizing more modern bonding ideas that reflect the electron-deficient cluster bonding first generalized with Wade's rules.[4] On the other hand, many of these phases show metallic and sometimes Pauli-like paramagnetism, indicating that some of the least bound valence electrons are unpaired and not fully localized.[5]

The K−Tl system alone contains numerous phases with structurally characterized clusters and networks. The K-richest, $K_{10}Tl_7$,[6] contains the unusual pentagonal-bipyramidal and apparently closed shell Tl_7^{7-} clusters but with an excess of potassium, apparently for packing reasons. The KTl analogue of the famous Zintl stuffed diamond type phase NaTl contains not the tetrahedra bonding of the stuffed diamond structure but, evidently because of relative atom sizes, approximately tetragonally compressed thallium octahedra in K_6Tl_6.[7] The next K_8Tl_{11} (as well as the Rb and Cs isotypes) contains novel Tl_{11}^{7-} pentacapped trigonal-pyramidal (D_{3h}) clusters, again, with one excess cation.[8,9] Isotypic examples are also known for In and Ga. Hetero-metal-centered thallium clusters (e.g., $Tl_{10}Zn^{8-}$, D_{4d}), and a variety of those that are found only in the presence of mixed cations (e.g., Tl_9^{9-}, $\sim C_{2v}$), will not be elaborated here.[3] It seems quite likely that further examples of discrete clusters

* To whom correspondence should be addressed. E-mail: jdc@ameslab.gov.
† Max Planck Inst. für Kohlenforschung, Mülheim, Germany.
‡ National Institute for Materials Science, Tsabuba, Japan.
§ Department of Chemistry, Montana State University, Bozeman, MT.

(1) This research was supported by the Office of the Basic Energy Sciences, Materials Sciences Division, U.S. Department of Energy (DOE). The Ames Laboratory is operated for DOE by Iowa State University under Contract W-7405-Eng-82.

(2) Belin, C. H. E.; Tillard-Charbonnel, M. *Prog. Solid State Chem.* **1993**, *22*, 59.
(3) Corbett, J. D. *Angew. Chem., Int. Ed.* **2000**, *39*, 670.
(4) Wade, K. *Adv. Inorg. Chem. Radiochem.* **1976**, *18*, 1
(5) Corbett, J. D. In *Chemistry, Structure and Bonding of Zintl Phases and Ions*; Kauzlarich, S. M., Ed.; VCH: New York, 1996,; Chapter 4.
(6) Kaskel, S.; Corbett, J. D. *Inorg. Chem.* **2000**, *39*, 778.
(7) Dong, Z.-C.; Corbett, J. D. *J. Am. Chem. Soc.* **1993**, *115*, 11299.
(8) Blase, W.; Cordier, G.; Müller, V.; Häussermann, U.; Nesper, R. *Z. Naturforsch. B* **1993**, *48*, 754.
(9) Dong, Z.-C.; Corbett, J. D. *J. Cluster Sci.* **1995**, *6*, 187.

10.1021/ic020667h CCC: $25.00
Published on Web 02/14/2003

will be found when compositional variables and reaction conditions are further explored.

Thallium-richer compositions give rise to network components. The novel $A_{15}Tl_{27}$, A = Rb, Cs, contains both discrete Tl_7^{7-} clusters and polythallium layers that can be imagined to result from the condensation of these units.[10] One complex result, the cubic $K_{49}Tl_{108}$, contains icosahedra and can be described in terms of samson polyhedra.[11] (However, this phase was prepared in an Al_2O_3 crucible, and its apparent composition deduced by crystallography has not been verified.) Another phase is the incompletely characterized $K_{23}Tl_{54}$.[12] Finally, the rather complex K_6Tl_{17} that separates from Tl-richer solutions on cooling is reported and described here.

Experimental Section

Syntheses. The stable phase K_6Tl_{17}, first evidenced following exploratory reactions in thallium-rich K−Tl systems, was synthesized in high yield once its composition and incongruent melting property were realized. Silvery chunks and crystals of K_6Tl_{17} were thus obtained in high yield via fusion of the elements in stoichiometric proportions in sealed Ta containers at 400 °C followed by quenching in water (to maintain a finely divided mixture of the components) and subsequent annealing at 150−200 °C for one month. Crystals of the compound, along with excess Tl, were similarly obtained from Tl-richer samples (K_6Tl_{18} to KTl_4) that had been quenched and then annealed at 200 °C and 5 d or 3 weeks at 150 °C. As usual, the welded Ta containers were protected from moisture and oxygen contamination by sealing them under vacuum within fused silica containers, all transfers and manipulations of samples were performed in a glovebox, and phase identification, proportions, and lattice dimensions were obtained from Guinier powder data. The compound readily decomposes in air to a gray-black material that contains mainly crystalline Tl metal according to the powder pattern.

Properties. The magnetic susceptibility of 49.9 mg of a high yield product of the compound was measured at a field of 3 T over the range 6−300 K on a Quantum Design MPMS SQUID magnetometer. The sample was held between two fused silica rods that were fixed inside a closely fitting silica tube and sealed at both ends under He. The raw magnetic data were corrected for the susceptibility of the container and the diamagnetism of the atomic cores. Electrical resistivities of the phase were measured by the electrodeless Q method on 54.8 mg of the compound that had been sieved to a 250−425 μm powder and diluted with chromatographic Al_2O_3. Measurements were made at 34 MHz over 98−270 K.

Diffraction Studies. Crystals of the compound were sealed in capillaries within a N_2-filled glovebox and checked for singularity with Laue photographs. The complete structure was solved and refined twice, the more precise result being accomplished with X-ray intensity data measured at 23 °C over the entire reciprocal sphere to $2\theta = 46.6°$ with the aid of a SMART1000 CCD-based X-ray diffractometer system and Mo Kα radiation. A total of 1845 frames was collected with an exposure time of 30 s/frame. The frames were integrated with the Siemens SAINT software package. The integration of the data for the indicated C-centered orthorhombic unit cell yielded a total of 17375 reflections of which 2277 were independent ($R_{int} = 0.083$) and 1322 were more intense than $4\sigma_F$. Final unit cell dimensions of $a = 16.625(1)$ Å, $b = 23.594(2)$ Å, $c = 15.369(2)$ Å were obtained from least squares refinement of 56 lines in the Guinier powder pattern that included diffraction lines from NIST silicon as an internal standard. Data were corrected for the sizable absorption ($\mu = 91.3$ mm^{-1}) with the aid of the SADABS program, which gave a relative transmission coefficient range 0.172−1.00.

Table 1. Some Crystal and Refinement Data for K_6Tl_{17}

fw	3708.89
cryst syst, space group, Z	orthorhombic, *Cccm* (No. 66), 8
unit cell dimens (Å, Å^3)[a]	
a	16.625(1)
b	23.594(2)
c	15.369(2)
V	6029(1)
d_{calcd}, g/cm^3	8.173
abs coeff μ (Mo Kα, mm^{-1})	91.297
R1, wR2 [$I > 2\sigma_I$][b]	0.059, 0.136

[a] Guinier powder data, $\lambda = 1.540562$ Å, 23 °C. [b] $R1 = \sum||F_o| - |F_c||/\sum|F_o|$, $wR2 = \{\sum[w(F_o^2 - F_c^2)^2]/\sum[w(F_o^2)^2]\}^{1/2}$.

Table 2. Fractional Atomic Coordinates ($\times 10^4$) and Equivalent Isotropic Displacement Parameters (Å$^2 \times 10^3$) for K_6Tl_{17}

atom	symmetry	x	y	z	U_{eq}[a]
Tl1	1	767(1)	484(1)	3234(1)	28(1)
Tl2	2/*m*	0	0	0	33(1)
Tl3	2	0	1638(1)	2500	33(1)
Tl4	222	0	5000	2500	45(1)
Tl5	1	1144(1)	0858(1)	1177(1)	33(1)
Tl6	1	753(1)	2782(1)	3273(1)	31(1)
Tl7	1	835(1)	3772(1)	1822(1)	34(1)
Tl8	*m*	116(2)	3216(1)	0	30(1)
Tl9	1	1198(1)	2379(1)	1207(1)	37(1)
Tl10	1	981(1)	4163(1)	3922(1)	32(1)
Tl11	*m*	767(2)	4567(1)	0	41(1)
Tl12	*m*	3101(2)	8067(1)	0	40(1)
K1	*m*	2696(9)	1550(6)	0	35(4)
K2	*m*	2769(1)	5277(7)	0	40(4)
K3	*m*	4440(1)	6647(6)	0	42(4)
K4	1	2258(7)	1651(4)	2862(8)	38(3)
K5	2	2767(1)	0	2500	51(5)

[a] U_{eq} is defined as one-third of the trace of the orthogonalized U_{ij} tensor.

The structure was solved and refined using the Siemens SHELXTL(Version 5.1) software package. The Tl atom positions were obtained by direct methods for the indicated space group *Cccm* (No. 49). The remaining potassium positions were obtained by subsequent analysis of the difference Fourier map. The final anisotropic refinement on F^2 converged at R1 = 5.9% and wR2 = 13.6%. The largest residual was 2.4 e/Å^3. Some general parameters and the atomic coordinates and displacement data are given in Tables 1 and 2. Distances appear in Table 3.

Theoretical Calculations. A full band empirical calculation (EHTB) on the anionic portion of the structure was carried out with the aid of the program CAESAR[13] with the Tl parameters (H_{ii}, eV, ξ) of 6s, 11.6, 2.30; 6p, 5.8, 1.6. Because of the large number of independent atoms (136) and orbitals, the calculation of the Tl−Tl COOP curve only was limited to atoms within the layers (117), that is, excluding the interlayer bridging Tl12.

Results and Discussion

Structure. K_6Tl_{17} has a unique layered structure that can be derived from the Cr_3Si structure type through reduction

(10) Dong, Z.-C.; Corbett, J. D. *Inorg. Chem.* **1996**, *35*, 1444.
(11) Cordier, G.; Müller, V. *Z. Naturforsch.* **1993**, *48b*, 1035.
(12) Dong, Z.-C.; Corbett, J. D. Unpublished.
(13) Hyde, G. B.; Andersson, S. *Inorganic Crystal Structures*; J. Wiley and Sons: New York, 1989; p 356.

Table 3. Bond Distances in K_6Tl_{17} (Å)

Tl1−Tl1	3.208(4)	Tl9−Tl6	3.396(3)
Tl1−Tl2	3.209(2)	Tl9−Tl6	3.473(3)
Tl1−Tl3	3.211(3)	Tl9−Tl7	3.473(3)
Tl1−Tl5	3.341(3)	Tl9−K4	3.54(1)
Tl1−Tl5	3.352(2)	Tl9−Tl5	3.589(3)
Tl1−Tl1	3.403(4)	Tl9−K1	3.63(1)
Tl1−Tl5	3.420(3)	Tl9−K1	3.67(1)
Tl1−Tl1	3.421(4)	Tl9−Tl9	3.711(4)
Tl1−K2	3.68(1)	Tl9−K3	3.87(2)
Tl1−K5	3.69(2)	Tl10−Tl10	3.313(4)
Tl1−K4	3.75(1)	Tl10−Tl7	3.357(3)
Tl1−K3	3.88(1)	Tl10−Tl7	3.365(3)
Tl2−Tl1 ×4	3.209(2)	Tl10−Tl4	3.367(2)
Tl2−Tl5 ×4	3.316(2)	Tl10−Tl6	3.427(2)
Tl2−K2 ×2	3.77(2)	Tl10−Tl12	3.429(3)
Tl2−K3 ×2	4.00(2)	Tl10−Tl11	3.444(3)
Tl3−Tl6 ×2	3.205(3)	Tl10−Tl11	3.478(3)
Tl3−Tl1 ×2	3.211(3)	Tl10−K5	3.61(1)
Tl3−Tl9 ×2	3.313(2)	Tl10−K2	3.65(2)
Tl3−Tl5 ×2	3.336(2)	Tl10−K4	3.86(1)
Tl3−K4 ×2	3.80(1)	Tl11−Tl11	3.269(6)
Tl3−K3 ×2	3.954(4)	Tl11−Tl8	3.367(4)
Tl4−Tl10 ×4	3.367(2)	Tl11−Tl7 ×2	3.373(2)
Tl4−Tl7 ×4	3.377(2)	Tl11−Tl10 ×2	3.444(3)
Tl4−K5 ×2	3.712(16)	Tl11−Tl10 ×2	3.478(3)
Tl5−Tl2	3.316(2)	Tl11−K1	3.67(2)
Tl5−Tl3	3.336(2)	Tl11−K2	3.73(2)
Tl5−Tl1	3.341(3)	Tl12−Tl6 ×2	3.335(3)
Tl5−Tl1	3.352(2)	Tl12−Tl8	3.368(14)
Tl5−Tl1	3.420(3)	Tl12−Tl12	3.340(6)
Tl5−K1	3.55(1)	Tl12−Tl10 ×2	3.429(3)
Tl5−Tl9	3.589(3)	Tl12−K4 ×2	3.63(3)
Tl5−Tl5	3.619(4)	Tl12−K3	4.02(1)
Tl5−K4	3.69(1)	K1−Tl5	3.55(1)
Tl5−K2	3.70(1)	K1−Tl9 ×2	3.63(1)
Tl5−K3	3.84(2)	K1−Tl9	3.67(1)
Tl5−K5	3.94(1)	K1−Tl11	3.67(2)
Tl6−Tl8	3.190(2)	K1−Tl8	3.68(2)
Tl6−Tl7	3.231(3)	K1−Tl7 ×2	3.79(1)
Tl6−Tl12	3.335(3)	K2−Tl7 ×2	3.651(1)
Tl6−Tl9	3.396(3)	K2−Tl1	3.68(1)
Tl6−Tl10	3.427(2)	K2−Tl5 ×2	3.70(1)
Tl6−Tl6	3.451(4)	K2−Tl11	3.73(2)
Tl6−Tl9	3.473(3)	K2−Tl2	3.77(2)
Tl6−Tl7	3.527(3)	K2−K5	3.998(6)
Tl6−K4	3.62(1)	K3−Tl6	3.78(1)
Tl6−K4	3.71(1)	K3−Tl5 ×2	3.84(2)
Tl6−K3	3.78(1)	K3−Tl8	3.87(2)
Tl7−Tl8	3.316(2)	K3−Tl9 ×2	3.87(2)
Tl7−Tl10	3.357(3)	K3−Tl1	3.88(1)
Tl7−Tl10	3.365(3)	K3−Tl3 ×2	3.954(4)
Tl7−Tl4	3.372(2)	K3−Tl12	4.02(1)
Tl7−Tl11	3.373(2)	K4−Tl9	3.54(1)
Tl7−Tl7	3.470(4)	K4−Tl6	3.62(1)
Tl7−Tl9	3.473(3)	K4−Tl12	3.63(1)
Tl7−Tl6	3.527(3)	K4−Tl7	3.68(1)
Tl7−K4	3.68(1)	K4−Tl3	3.80(1)
Tl7−K1	3.79(1)	K4−Tl10	3.86(1)
Tl7−K5	3.86(1)	K4−K5	4.02(1)
Tl8−Tl6 ×2	3.190(2)	K4−K4	4.09(2)
Tl8−Tl9	3.252(3)	K5−Tl10 ×2	3.69(1)
Tl8−Tl7 ×2	3.316(2)	K5−Tl1	3.69(2)
Tl8−Tl10 ×2	3.326(3)	K5−Tl4	3.71(2)
Tl8−Tl11	3.367(4)	K5−Tl7 ×2	3.89(1)
Tl8−Tl12	3.368(4)	K5−Tl5	3.94(1)
Tl8−K1	3.68(2)	K5−K2	3.998(6)
Tl8−K3	3.87(2)	K5−K4	4.02(1)
Tl9−Tl8	3.252(3)		
Tl9−Tl1	3.313(2)		

and introduction of both extra Tl atoms and cation spacers. The basic building blocks are the idiosyncratic *tetrahedral stars* (stella quadrangula[13] or tetraederstern[14]). This is a common building block in intermetallic phases[15] and may be simply described in terms of an inner tetrahedra, ideally T_d, that is further face-capped, often by the same element, to generate a second, larger inverted tetrahedron. The variety of such examples is large, especially among electron-poorer examples (VEC = 2.1−2.6).[15] (This article includes a note that condensed double tetrahedral stars can be recognized in the construction of the peculiar thallium layer reported before in $A_{15}Tl_{27}$, A = Rb, Cs.[10])

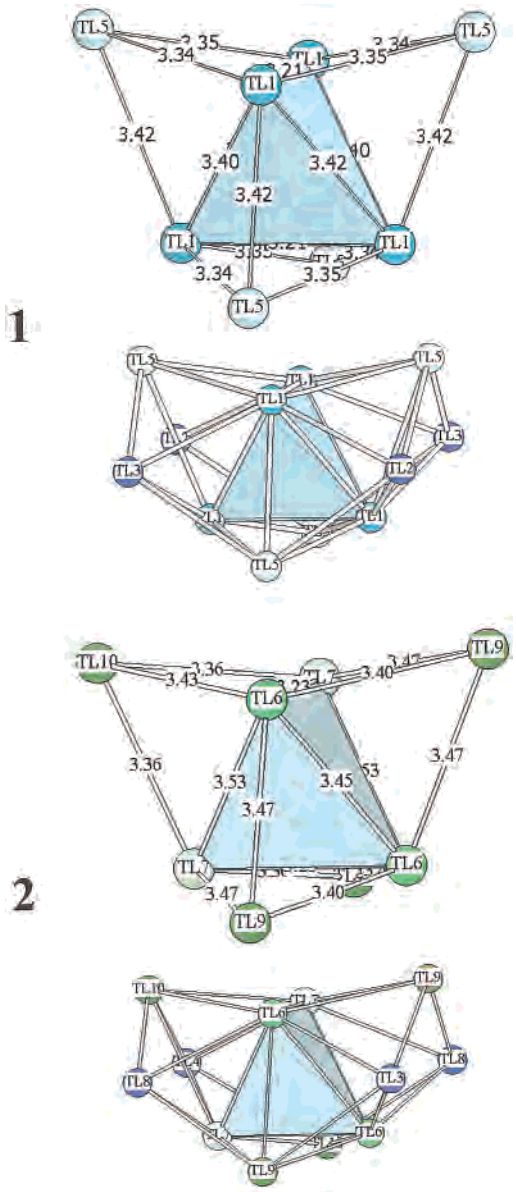

Figure 1. The 8-atom stars and their augmented 12-atom polyhedra in K_6Tl_{17}. Top, star 1; bottom, star 2. The color key is given in the caption for Figure 2.

The K_6Tl_{17} structure contains two distinct types of tetrahedral stars, and in contrast to Cr_3Si, each is augmented with four additional Tl atoms that function as bridges to other stars. These constructions are shown in Figure 1. In star 1 (shades of blue), Tl1 and Tl5 define the inner and outer tetrahedra, respectively. The unit is centered at $(0,0,{}^1/_4)$ and

(14) Andersson, S. *Acta Crystallogr.* **1978**, *A34*, 833.

(15) Häussermann, U.; Svensson, C.; Lidin, S. *J. Am. Chem. Soc.* **1998**, *120*, 3867.

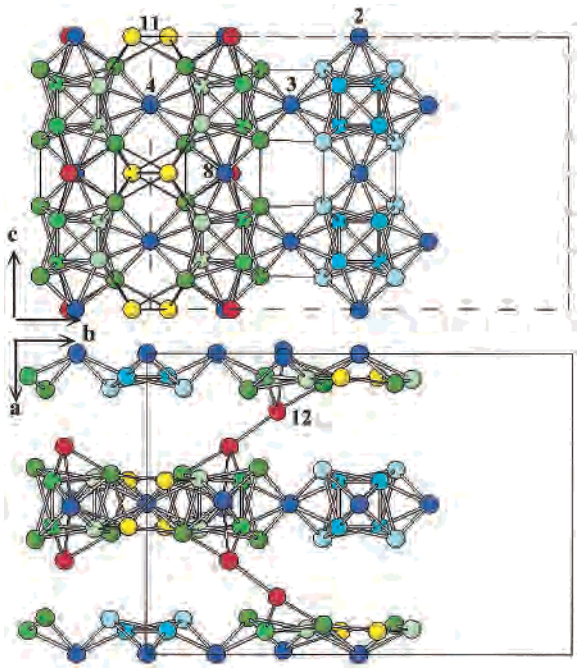

Figure 2. (a) The independent portion of one layer around $x = {}^1/_2$ in K_6Tl_{17} [001]. (b) [001] view of portions of three layers and their interbridging by Tl12 dimers. [Star 1: Tl1, blue; Tl5 (outer), light blue; augmenting Tl2, 3, dark blue. Star 2: Tl6, green; Tl7, light green; Tl9, 10 (outer), dark green; augmenting Tl4, 8, dark blue; interstar 2 bridging Tl11 dimers, yellow; interlayer bridging Tl12 dimers, red.]

has 222 (D_{2d}) symmetry, a subset of the proper tetrahedral elements, with modest distortions from T_d (d(Tl−Tl) = 3.21−3.42 Å). This unit is further augmented by a square of Tl2 (2/m) and Tl3 (2) atoms (both dark blue) that cap the four quadrilateral faces around the waist of the basic star, as shown in the second part of Figure 1 (3.21−3.34 Å added). The less symmetric star 2 (greenish) is centered at (0, 0.67, ${}^1/_4$) and consists of Tl6 and 7 as the inner tetrahedron and Tl9 and 10 as the outer (d(Tl−Tl) = 3.23−3.53 Å). Its only symmetry is a single 2-fold axis that bisects the Tl6−Tl6 and Tl7−Tl7 edges of the former. This unit is further bonded to four interstar bridging atoms (dark blue), one Tl3 (sym 2), one Tl4 (222), and two Tl8 (m) (3.19−3.38 Å added). The atom color coding scheme employed within the stars in Figure 1 is also listed in the legend to Figure 2.

The interconnection of these two stars in 1:2 proportions together with a few additional Tl atoms generate the layered anionic lattice in K_6Tl_{17}. Somewhat more than one independent unit is shown in Figure 2 in two views, normal to the layers [100] at the top and parallel to these layers at the bottom ([001]). Stars 1 and 2 are color coded in shades of blue and green, respectively, and the augmenting Tl2, 3, 4, and 8 atoms on these that link the clusters into layers are dark blue. Two additional and rather remarkable diatomic links are also present, pairs of Tl11 atoms (yellow) that participate in the interconnection of four type 2 clusters, and Tl12 dimers (red) that directly link the cluster layers together along the $\vec{a}$ direction. The clusters are again emphasized by broader "bonds", and all Tl−Tl bonds up to 3.53 Å are marked by these open bonds. (The separations range down to 3.19 Å, with most falling below 3.40 Å.) All Tl atoms have between six and nine like neighbors, so the bonding is

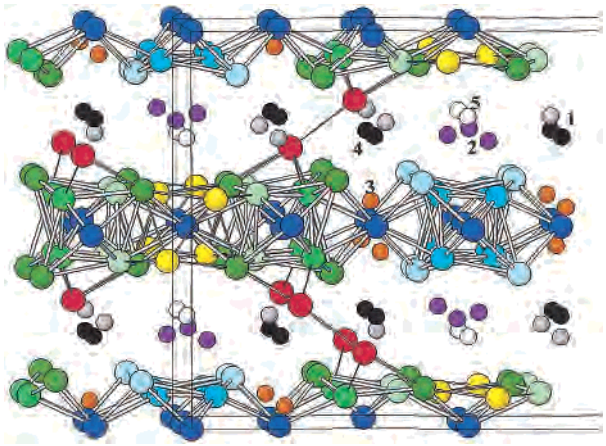

Figure 3. [001] view of the structure of K_6Tl_{17} that includes the (smaller) potassium positions in the interlayer regions. K1, gray; K2, purple; K3, orange; K4, black; K5, white.

typically electron deficient (see later). The notable Tl5 and Tl9 atoms with only six Tl neighbors surround the open area around ∼0.4, ∼${}^1/_3$, ${}^1/_2$ that is defined by lighter lines in Figure 2a. Although the separations in this rectangle are somewhat above the 3.53 Å cutoff used for heavier "bonds", namely, 3.59 and 3.71 Å, these still represent significant bonding. Likewise, the cation placements in this region are also important; both will be considered shortly.

The cation placements about and between the single anion layer and parts of the two symmetry related adjoining slabs in Figure 2b are illustrated in Figure 3 (slightly rotated). All of these have complementary orientations and functions with respect to adjoining layers, and it is clear that close cation contacts exist for all thallium atoms, appropriate for this basically ionic component of the total stability of this phase. But the unevenness in the distributions also reflects details in this complex structure. The color coding of the cations given in the caption to Figure 3 together with distances in Table 3 will enable the interested reader to identify all of the contacts in detail. One functional contrast is the largely intralayer bonded K3 (orange) which lies fore-and-aft of the intercluster bridging Tl3 in this view at a longer distance, 3.95 Å. This puts K3 in the open rectangle just noted where it makes several contacts with atoms in the neighboring clusters in the same layer, Tl6, Tl5 (×2), Tl9, and Tl1, and also contacts a Tl12 atom below on the neighboring layer (4.02 Å). In parallel, K1 (gray) lies above and below this rectangle with close neighbors of Tl5, Tl9 (×2), and the Tl3 bridge, and it also contacts four Tl atoms on the neighboring layer, directly above the bridging Tl8 plus the neighboring Tl7, Tl9, and Tl11. Analogous roles can be deduced for K4 (above and below star 2), K5 (above the bridging Tl4 and star 1), and K2 (above and below the Tl11 pairs and the bridging Tl3). As expected in this type of saltlike phase, coulomb energies must play a major role in determining its composition and stability, above and beyond the (probably modest) strengths of the covalent Tl−Tl bonds emphasized in the drawings.

Variations in the number of contacts about each thallium and potassium are distinctive and characteristic, Table 4. Tl8 has the largest number of Tl neighbors, nine, because one

Table 4. Atom Contacts, Charges, and Tl−Tl Overlap Populations

atom	Tl contacts[a]	K contacts	sum	charge[b]	∑OP/atom	$\overline{\text{OP}}$ per neighbor
Tl1	8	3	11	−0.38	**2.183**	0.272
Tl2	8	2	10	−0.12	**2.528**	0.316
Tl3	8	2	10	−0.14	**2.556**	0.320
Tl4	8	2	10	−0.15	**2.184**	0.273
Tl5	7	3	10	−0.71	1.942	0.277
Tl6	8	3	11	−0.15	1.945	0.243
Tl7	8	3	11	−0.28	1.780	0.224
Tl8	**9**	**2**	11	**0.19**	1.982	0.220
Tl9	**6**	**4**	10	−0.63	1.770	0.295
Tl10	8	3	11	−0.25	2.008	0.251
Tl11	8	2	10	−0.33	**2.364**	0.296
Tl12	**6**	2	**8**	−0.82	**2.226**	**0.371**
K1	8					
K2	7					
K3	7[c]					
K4	6					
K5	6					

[a] Ranges used: Tl−Tl, 3.19−3.62 Å; K−Tl, 3.54−3.90 Å. Noteworthy results are bold-faced. [b] From EHTB calculations on anion lattice. [c] Contacts counted include 6 distances > 3.80 Å, and there are 3 more with $3.95 < d \leq 4.02$ Å.

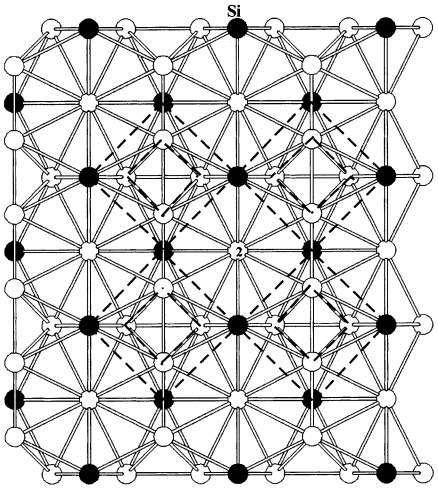

Figure 4. Layer in cubic Cr_3Si with tetrahedra stars emphasized (Cr, white; Si, black).

member of the interlayer Tl12 dimer lies directly below or above Tl8. This in turn appears to limit Tl8 to only two cation neighbors in the range used in Table 4, at 3.68 and 3.87 Å. (This environment presumably also accounts for the unusual charge distribution on Tl8 described later.) On the other hand, lower numbers of Tl−Tl bonds about other thallium atoms parallel increased numbers of K contacts within the selected distance limits, as for Tl5 (7 Tl−Tl, 3 Tl−K) and Tl9 (6, 4), atoms about which the unusual environments in the open rectangle have already been noted. The three 8 Tl + 3 K neighbor examples (Tl6, 7, 10) do not seem so unusual, but a special and contrasting situation applies to Tl12 (6, 2) in the isolated dimers. This unusual feature will be considered later along with computed overlap populations.

For comparison, Figure 4 shows one layer in the simpler structure of the somewhat distant parent Cr_3Si, in which chromium atoms (white) constitute the inner and silicon atoms (black) the outer tetrahedra in the stars. But in contrast to K_6Tl_{17}, the basic layers are flat, not puckered, and the 3-dimensional cubic structure is made up from ideal tetrahedral stars that share outer (Si) atoms directly. Four of the stars are outlined in Figure 4 (Si, ●; Cr, ○) for comparison with Figure 2a. Note that the chromium atoms lie in three nonintersecting chains parallel to the cell axes, the third one normal to the figure appearing as a Cr atom centering a hexagonal antiprismatic cavity $[(Cr_4Si_{4/2})Cr_2]$.

In contrast, the homoatomic anionic layers in K_6Tl_{17} contain rotated and distorted tetrahedral stars that are additionally surrounded by a square arrangement of augmenting Tl atoms (dark blue, Tl2, 3, 4, 8) that cap the quadrilateral faces around the waist of each star. Distortions of the stars give rumpled, not planar, faces to the layers. The same types of stars are interconnected by Tl2, Tl4, or Tl8 whereas Tl3 provides a link between different types of stars (Figure 2a). Additional Tl11 dumbbells (yellow) aid the condensation of four adjacent star 2 cluster units by binding to Tl7 and Tl10 therein whereas the analogous position between star 1 and star 2 is filled by Tl3 (plus K3 and K1 below). However, Tl12 dumbbells also link the layers together; these atoms are tightly bonded to each other and to Tl8 and two pairs of Tl6 and Tl10 atoms above or below, all in the range 3.34−3.43 Å. The complexity of the overall polyanion clearly reflects the presence of significant covalent bonding effects for thallium.

All potassium ions have large coordination numbers when tabulated to a larger 4.6 Å limit, from 14 for K1 up to 17 for K3. The K−Tl distances fall in a range between 3.55 and 4.28 Å, and K−K distances are 4.00 Å and above. The polyhedra about K2, K5 (CN 15), and K4 (CN 16) are distorted Frank−Kasper polyhedra whereas the environment of K1 (CN 14) is better described as a unicapped square prism of Tl atoms that is waist capped by four K ions, approximately in a square arrangement. The coordination of 17 atoms around K3 (3 K + 14 Tl) is quite rare in crystal chemistry.

At this point we also wish to point out that even Tl-richer phases occur with the larger cations Rb and Cs, namely, $A_4Tl_{12.8}$ (*Cmca*).[12] These exhibit a novel combination of both parallel 1-D chains built of condensed antiprismatic pentagonal prisms (strikingly similar to the Ta columns in Ta_2S and Ta_6S[16]) and 2-D puckered sheets of similar but defect pentagonal antiprismatic columns interconnected by distorted chains of tetrahedra. Additional thallium is partially disordered down the pentagonal antiprisms in both chains, and some Rb atoms appear to be substituted in a regular way in the second type of disordered Tl chain.

Properties and Bonding. The electrical resistivity of polycrystalline K_6Tl_{17}, 22.6 $\mu\Omega\cdot$cm (270 K), is quite low and comparable to that of Tl metal (16.4 $\mu\Omega\cdot$cm at 295 K[17]). Also the temperature coefficients are quite similar, K_6Tl_{17}, 0.34% K^{-1}; Tl, 0.29% K^{-1}. The measured Pauli-like paramagnetism (1.1×10^{-4} emu/mol at 296 K) is rather typical for this type of compound[5] and gives further evidence for the metallic character of the compound. Plots of both

(16) Franzen, H. F.; Smeggil, J. G. *Acta Crystallogr.* **1969**, *B25*, 1736; **1970**, *B26*, 125.
(17) *American Institute of Physics Handbook*, 3rd ed.; McGraw-Hill Book Co.: New York 1972; pp 9B39, 9B42.

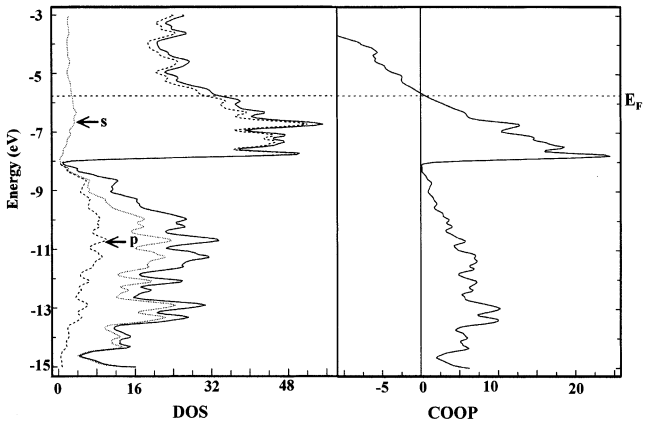

Figure 5. Left: densities-of-states vs energy (eV) for Tl_{17}^{6-} with Tl 6s (···) and 6p (- - -) projections marked. Right: COOP curve for a portion of the Tl_{17}^{6-} layers. E_F is marked with a dashed line.

properties as a function of temperature are contained in Supporting Information.

Band structure calculational (EHTB) results for the three-dimensional extended Tl_{17}^{6-} anionic net are in agreement with these properties. The densities-of-states given in Figure 5 show no band gap near the Fermi level. The nearby bonding states originate mainly from p-orbital interactions between the Tl atoms, which are clearly separated from the low lying s-like states. These contributions are emphasized in projections of s- and p-orbital contributions in the total DOS, the result of the larger energy difference between s- and p-states generally associated with the heavier post-transition elements (inert pair effect). The overlap-weighted COOP curve on the right side of Figure 5 for just the layer impressively shows that this metal-like compound still maximizes its bonding (positive Tl−Tl overlap) up to E_F, as valence compounds generally do.

Although distances are commonly used as rough measures of bond strengths, it is clear that these may be poor approximations in instances in which high symmetry, relative sizes, or particular electronic features of complex bonded networks may largely determine interatomic distances. These may be usefully termed "matrix effects". The first was initially discussed at some length for cluster systems,[18] whereas the second has been very evident more recently from studies of metal-rich binary and ternary scandium telluride systems. For example, the Sc−Sc bonds on the surface of Sc metal chains, networks, and so forth have distinctly lower Mulliken overlap population (OP) values relative to their distances, evidently because of Sc−Te covalent interactions around the outside of the metal arrays. Examples are found in Sc_8Te_3,[19] Sc_9Te_2,[20] and $Sc_5Ni_2Te_2$.[21]

Likewise noteworthy features and differences related to the bonding in the more complex K_6Tl_{17} structure can be found in its Tl−Tl OP data (Table S3, Supporting Information), which range between 0.03 and 0.54 for distances between 3.62 and 3.19 Å. In general, the strongest interactions lie on the surface of the shell-like Tl_{12} cluster units (augmented tetrahedral stars) and at the bridging atoms. On the other hand, bonding within both inner stars is relatively weak (OP < 0.2) except along the diagonals in both that are seen in projection in Figure 2a (OP > 0.3). Two-center populations between inner and outer star atoms are generally intermediate. Several strikingly large populations appear in bridging interactions around Tl2, Tl3, Tl11, and Tl12 but only once at Tl8 (Tl8−Tl9, 0.40) and Tl4 (Tl4−Tl10, 0.34). In general, there are many instances in this complex arrangement wherein the distances are not good indicators for the relative overlap populations and, presumably, something akin to bond strength. A clearer way[19−21] to sort out these anomalous features is via a plot of pairwise overlap populations versus observed distances in the structure (not shown). Particularly large OP values relative to distances occur for the Tl−Tl pairs 5−9, 6−12, and 12−12, and moderately high values occur for the intracluster 1−5, 6−9, and 7−9 and the bridging 4−10, 7−11, 10−11, and 11−11. On the other hand, a very weak interaction apparently occurs for the intracluster Tl6−Tl6. The frequency with which certain structurally special or unique atoms Tl5, Tl6, Tl9, Tl11, and Tl12 appear in these exceptions seems important. We have already had occasion to note special features of many of these atoms.

Although detailed explanations of these bonding irregularities and their interrelationships in such a complicated structure would require an investigation that is a great deal deeper than we wish to undertake, the large number of independent atoms is apt to deter any more thorough investigation. Some summary data in Table 4 emphasize the important points. The approximate (negative) charge distribution on the Tl atoms in the anionic lattice should logically mirror the cation distribution, and the three most negative (> −0.5) atoms, Tl5, Tl9, and Tl12, are those with the smaller number of Tl bonds and, in part, a larger number of cation neighbors. (Our counting here is simple, without any sophistication in weighting K−Tl distances over the range 3.55−3.90 Å.) The somewhat odd member is again the Tl12 atom. The second group of charges involves Tl1, Tl7, and Tl10, all with three cation neighbors, and the unusual Tl11. The opposite extreme, a striking charge of about +0.19 e^- for Tl8, is more or less consistent with the presence of the ninth interlayer Tl12 neighbor that shields it from other cations.

Sums of overlap populations per Tl atom, Table 4, column 6, give a quick reflection of total Tl−Tl bonding per center, the greater (>2) occurring for the bridging Tl2, 3, and 4, the inner cluster Tl1, and, again, the novel bridging Tl11 and Tl12, the last one despite only six Tl−Tl bonds. The last column in the table, which gives the average Tl−Tl OP per Tl neighbor, levels these out pretty well (0.22−0.32) save again for the very high values (0.37) about the unique Tl12.

We have in the foregoing attempted to (1) describe and (2) understand something about the nature of the relatively complex structure of K_6Tl_{17}. This compound in itself falls in a class of "polar intermetallics" for which the nature of

(18) Corbett, J. D. *J. Solid State Chem.* **1981**, *37*, 335.
(19) Maggard, P. A.; Corbett, J. D. *Inorg. Chem.* **1998**, *37*, 814.
(20) Maggard, P. A.; Corbett, J. D. *J. Am. Chem. Soc.* **2000**, *122*, 838.
(21) Maggard, P. A.; Corbett, J. D. *Inorg. Chem.* **1999**, *38*, 1945.

the structures and bonding might already seem rather unfamiliar. Nonetheless, we can find some consistent features or sensibilities among the bonding in this class of triel (Ga, In, Tl) compounds in general, recognizing that the coulomb interactions in this kind of "salt" must play a large role in selection and stability of the chosen structure.[3−5] We have played this interpretative role fairly boldly in the present article, despite the complexity of the structure and the variety of bonding situations. The latter features alone make it unlikely that any higher level theoretical inquiry will be considered worthwhile.

Acknowledgment. We are indebted to Jerome Ostenson for the magnetic measurements.

Supporting Information Available: Tables of atom collection and refinement parameters, distances, and overlap populations and graphs of resistivity and magnetic susceptibility data. This material is available free of charge via the Internet at http://pubs.acs.org.

IC020667H